

## 1 The Role of Comets in the Late Heavy Bombardment

The Nice model describes a plausible scenario where the Jovian planets experienced a global instability that led to a reorganization of the outer solar system; planets moved, existing small body reservoirs were depleted or eliminated, and new reservoirs were created in distinct locations [1, 10]. The putative trigger for this event is thought to be gravitational interactions between the giant planets and a planetesimal disk of several tens of Earth masses residing just outside the initial orbits of the giant planets. This primordial disk, made of comet-like objects, was scattered throughout the solar system by planet migration.

The Nice model is compelling because it can quantitatively explain the orbits of the Jovian planets [10, 32], the capture of comets from the primordial disk into several different small body reservoirs in the outer solar system (e.g., Trojans of Jupiter [33] and Neptune [34], the Kuiper belt and scattered disk [35], the irregular satellites of the giant planets [36, 37], and the outer asteroid belt [38]). It has also been linked in time to the so-called Late Heavy Bombardment (LHB) of the Moon and terrestrial planets [1]. These accomplishments are unique among models of outer solar system formation.

The existence of the terrestrial planets on their current orbits, as well as the dynamical sculpting of the asteroid belt by sweeping resonances, also provide constraints for the Nice model. These issues have been explored in considerable detail by [11, 12, 17, 32, 39]. Their results provide an important context for our approach because they show that solutions for the Nice model can reproduce current conditions, provided that the giant planets migrate from their original orbits to their current orbits in less than 1 My.

A potential problem with the original Nice model, however, concerns its use of comets as a key component of the LHB in the inner solar system. This scenario may be discordant with the ancient crater size-frequency distributions (SFDs) found on Mercury, the Moon, and Mars. For example, [20] argue they closely resemble the SFDs of asteroids in the main belt, and not the crater SFDs found on the outer planet satellites<sup>1</sup>. If comets and asteroids indeed have contrasting SFDs, one can potentially use this difference to test the Nice model as well as set limits on the size of the LHB-era comet impactor population and/or the initial primordial disk population just before the LHB.

For this calculation, we assumed that comets contribute  $< 10\%$  of the ancient lunar crater populations produced by the LHB. Thus, their signature would presumably be mixed in and lost among the crater size frequency distribution produced by asteroids. The number of  $D > 20$  km craters found on the most ancient lunar surfaces is  $2\text{--}3 \times 10^{-4}$  km<sup>-2</sup>, while those on terrains near Nectaris basin are  $1 \times 10^{-4}$  km<sup>-2</sup> [28]. The surface area of the Moon is  $3.8 \times 10^7$  km<sup>2</sup>, while recently calculated impact probabilities between the Moon and test bodies scattered out of the primordial comet disk during the LHB are  $(8 \pm 3) \times 10^{-8}$  (e.g., [32]). Note that the lunar impact probabilities above may change as new variants of the Nice model are explored in additional detail. If we assume no comets disrupt en route to the inner solar system, the number of comets capable of making  $D > 20$  km lunar craters in the disk had to be limited to  $\sim 3 \times 10^9$  to  $\sim 2 \times 10^{10}$ . We call these values  $N_{\text{need}}$ .

The number of comets in the primordial disk at the time of the LHB can be roughly estimated by assuming that the Nice model made the scattered disk, the likely source of most Jupiter-family comets. As

---

<sup>1</sup>As an aside, we point out that recent work suggests that, when all factors are taken into account, comets hitting the Moon may actually have a main belt-like SFD (J. Richardson, personal communication). The distinguishing characteristic would be that the power law slopes of the cometary SFD are more extreme than those of a main belt-like SFD; that is, the steep branches of the cometary SFD are steeper than the main belt and the shallow branches are shallower. Further modeling is needed to determine whether such a SFD can easily be “hidden” when covered over by a younger main belt-like SFD.

estimated by [16], the number of kilometer-sized comets in the scattered disk is  $\sim 1 \times 10^9$ , with perhaps a factor of 5 uncertainty. The efficiency of placing primordial disk objects into the scattered disk has been estimated from numerical simulations to be  $\sim 4 \times 10^{-3}$  [40]. Together, they yield a range of  $\sim 5 \times 10^{10}$  to  $\sim 1 \times 10^{12}$ .

The comet size needed to make a  $D > 20$  km lunar crater is poorly known, but a reasonable estimate is  $D > 2$  km, based on standard cometary bulk densities of  $0.6 \text{ g cm}^{-3}$  [41], lunar impact velocities of  $25 \text{ km s}^{-1}$  [32], and Pi-group crater-scaling law relationships [30]. The size distribution of the primordial disk just before the LHB for 1 to 2 km diameter projectiles is unknown, but a conservative estimate is that the ratio of  $D > 1$  km comets to  $D > 2$  km comets is 2 to 4. Thus, this suggests the number of comets capable of making  $D > 20$  km lunar craters in the primordial disk just before the LHB ranged between  $\sim 1 \times 10^{10}$  to  $\sim 5 \times 10^{11}$ . We call this value  $N_{\text{estimate}}$ .

For LHB-era asteroid impactors to dominate comet impactors,  $N_{\text{estimate}} \leq N_{\text{need}}$ . Interestingly, the ranges of  $N_{\text{estimate}}$  and  $N_{\text{need}}$  slightly overlap, suggesting a potential solution set is possible. Still, it is fair to say that  $N_{\text{estimate}}$  is generally an order of magnitude higher than  $N_{\text{need}}$ . This could suggest the Nice model is wrong, comets produce a bigger component of lunar crater populations than suggested by [20], some of our above estimates/assumptions are inaccurate, or we are missing a physical mechanism that influences the calculation.

Concerning the latter possibility, it is well known that many comets disrupt en route to or while residing in the inner solar system (e.g., 57P/du Toit-Neujmin-Delporte; 73P/Schwassmann-Wachmann 3). The physical disruption of comets also provides the easiest way to deal with the so-called “fading problem” among nearly-isotropic comets, namely that models of the orbital evolution of new nearly-isotropic comets consistently predict far more returning comets than those observed [42]. By combining the orbital distribution of model comets with statistical models of dormant comet discoveries by well-defined surveys, and then comparing the model results to the observed population of dormant comets, [42] found that  $\sim 99\%$  of nearly-isotropic comets disrupt rather than become dormant. It is unknown whether a similar fraction of ejected primordial disk objects disrupt, but even a smaller fraction, say on the order of 90%, might be enough to satisfy  $N_{\text{estimate}} \leq N_{\text{need}}$ . New studies will be needed to determine whether such a disruption rate is reasonable for primordial disk comets at the time of the LHB.

Additional evidence can be brought to bear on the issue of whether asteroids or comets were a stronger source of LHB-era impactors. We briefly summarize two of these lines below.

- According to the dynamics of the Nice model, comets should strike the Moon over a window of several tens of My, while asteroids hit over hundreds of My [1] (see also main text). If comets dominated the LHB-era impact flux, we might expect the  $^{39}\text{Ar}$ - $^{40}\text{Ar}$  shock degassing ages among lunar samples and meteorites, which are presumed to be produced by impact heating, to be dominated by a narrow spike of ages [43]. Instead, measurements indicate lunar impact melts and heated samples returned by the Apollo astronauts have a wide range of ages between 3.7 and  $\sim 4.2$  Ga [22, 23]. The only pseudo-spike of ages occurs near 3.9 Ga, though some argue this could be a signature produced by the formation of Imbrium basin (e.g., [44]).  $^{39}\text{Ar}$ - $^{40}\text{Ar}$  ages from eucrites, most of which were likely derived from (4) Vesta, show a spike at 4.5 Ga, few ages between 4.1 and 4.4 Ga, and numerous ages between 3.3-4.1 Ga (e.g., [24]). H chondrites show a similar pattern: 7 events between 3.5-4.1 Ga and no events in the intervals between 4.1-4.4 Ga and 1.5-3.5 Ga [24, 45].
- When large projectiles strike the Moon, they often produce impact melts containing highly siderophile elements (HSEs) derived from the impactor. So far, studies of such HSEs from Apollo samples show little affinity for CI or CM meteorites, a reasonable proxy for comet-like projectiles (e.g., see [21] and numerous references therein). Suggested matches include enstatite chondrite-like objects, iron

meteorites, and perhaps ordinary or even CV chondrites. With this said, it is plausible that the available HSE signatures are dominated by a few basin-forming impacts that occurred near the Apollo landing sites (e.g., Imbrium, Serenitatis).

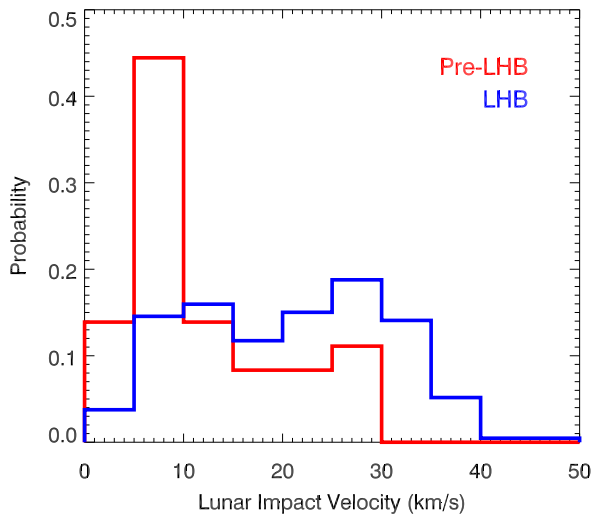


Figure S1: The impact velocity distribution of E-belt asteroids on the Moon. They were calculated from the orbital parameters of the test bodies that struck in the Earth in the combined  $e_{\max}^{\text{Mars}} = 0.025, 0.05, 0.12, \text{ and } 0.17$  runs. No significant changes were seen between the runs. The velocity distribution for the pre-LHB-era was based on 36 impact events, while the LHB-era was based on 213 events. The mean and median velocities at in the Pre-LHB were  $V = 11.9 \pm 8.1$  and  $8.6 \text{ km s}^{-1}$ , while those for the LHB were  $V = 20.7 \pm 9.8$  and  $20.9 \text{ km s}^{-1}$ .

## 2 Basin-Sized Projectiles in the Hungaria Population

In order to constrain the original E-belt population, we estimated the number of asteroids capable of producing lunar basins in the present-day Hungaria asteroid population. This was done as follows.

First, we considered the Hungaria family, which includes (434) Hungaria and numerous E-type asteroids [14, 15], separately from the background population. Using the family's absolute magnitude distribution as derived by [14], and assuming an albedo of 0.38 for all family members, we derived the family's size-frequency distribution (SFD). These results were compared to the results of numerical impact experiments created using a smooth particle hydrodynamic (SPH) code coupled to an  $N$ -body code. As described by [46], these impact experiments followed projectiles shot into coherent target asteroids over a wide range of projectile/target mass ratios, collision velocities, and impact angles. The resultant model SFDs can be directly compared to the largest bodies of the derived SFD described above, mainly because these objects have yet to experience significant collisional evolution. Because the model SFD must explicitly conserve mass down to the code's resolution limit, a reasonable match at the large diameter end of the SFD allows us to estimate how much of the parent body's mass was initially in the form of smaller objects. Our results indicate the E-type Hungaria family probably represented a single  $D > 40 \text{ km}$  asteroid. Note that a LHB-era projectile of this size would be capable of making an Orientale-sized basin on the Moon [30].

Second, we examined the background Hungaria population. It contains a diverse set of objects made up of E-, X-, S-, and C-type bodies [14]. The shape of the absolute magnitude distribution of the background Hungarias was shown in [14]. We converted these objects into diameters by assuming 45% were S-type asteroids, with mean albedos of 0.20, and 45% were E-type asteroids, with mean albedos of 0.38. For the remaining low-albedo objects, we directly included the diameters of the largest known objects as determined by IRAS observations [14].

As part of this calculation, we computed the lunar impact velocity distribution of E-belt objects with the Moon using the runs described in the main text (Fig. S1). The LHB-era velocity distribution of E-belt projectiles is broad, such that no single value adequately characterizes it (i.e., mean impact velocity  $V$  of  $21 \pm 10 \text{ km s}^{-1}$ ; median  $V$  of  $21 \text{ km s}^{-1}$ ). For this reason, we created an impact code that allowed our calculated SFDs to hit the Moon at all possible impact velocities, with the probability associated with a given  $V$  used to weight the likelihood that a particular projectile would create a basin. The bulk densities of the impactors were assumed to be  $2.7$  and  $1.3 \text{ g cm}^{-3}$  for bright and dark asteroids, respectively. Finally, all of our values were input into the Pi-group crater-scaling law relationships described by [30]. Taking all of these components together, we estimate there are roughly  $4 \pm 2$  asteroids in the Hungaria population capable of making diameter  $D_{\text{crat}} > 300 \text{ km}$  basins on the Moon.

### 3 Small Number Statistics and the Initial E-belt Population

We find it interesting that only  $4 \pm 2$  basin-forming projectiles are left in the Hungarias after 4 Gy of evolution, while the original E-belt population was potentially  $\sim 1000$  times larger. This kind of extreme depletion raises the possibility that small number statistics in the current Hungarias have affected our estimates of the initial E-belt population. To glean insights into this, we created a Monte Carlo code capable of tracking asteroid losses in the Hungaria population over the last 2.1 Gy.

Here we assumed that  $N$  was the number of Hungarias large enough to make a lunar basin at time  $t$ , where  $t = 0 \text{ My}$  is defined as the start of the LHB. The mean value of  $N$  at  $t = 2000 \text{ My}$  was defined as  $N_{\text{init}}$ , while the mean value of  $N$  at  $t = 4100 \text{ My}$  (i.e., today's value) was defined as  $N_{\text{ave}}$ . Next, we calculated the mean decay rate of the  $e_{\text{max}}^{\text{Mars}} = 0.025$  run between  $t = 2000$  and  $4100 \text{ Gy}$ . By combining this value with  $N_{\text{ave}}$ , we estimated  $N_{\text{init}}$ . These values were input into our Monte Carlo code, which was started at  $t = 2000 \text{ My}$  with the Hungaria population having  $N_{\text{init}}$ . Then, at every 1 My timestep, we used random deviates to determine whether individual Hungaria asteroids would be eliminated according to the expected asteroid decay rate. The number left at  $t = 4100 \text{ Ma}$  was called  $N_{\text{final}}$ . For each Monte Carlo code run, we ran 1000 trials in order to determine a probability distribution of  $N_{\text{final}}$  values.

In our first Monte Carlo run, we assumed  $N_{\text{ave}} = 4$ . Over 1000 runs, we found a mean value of  $N_{\text{final}} = 4.3 \pm 3.3$ , matching  $N_{\text{ave}}$ . The probability of  $N_{\text{final}}$  being zero was 17% while the probability of being left with 8 or more asteroids was 11%. This provided us with a sense of the variability of our system. In our second Monte Carlo run, we assumed  $N_{\text{ave}} = 2$ . We found the probability of getting  $N_{\text{final}} \geq 4$  was  $\sim 20\%$ . In our third run, we set  $N_{\text{ave}} = 8$  and found a 26% chance of getting  $N_{\text{final}} \leq 4$ . All of these outcomes are reasonably probable.

Our interpretation of the Monte Carlo results is that our initial E-belt populations, as derived using (a)  $4 \pm 2$  basin-forming projectiles in the Hungarias and (b) the decay rates from Fig. 2 of the main text, could easily vary by an additional factor of 2 beyond what was calculated in the main text. This suggests that other constraints, such as those found in the lunar and terrestrial impact record, may be needed to more precisely quantify the starting E-belt population.

### 4 Lunar Basin Production Calculations

**LHB-era lunar basins from the primordial main belt.** Our estimate of  $3 \pm 2$  LHB-era lunar basins from the primordial main belt comes from the following components. We calculated that an asteroid of diameter  $D > 11 \text{ km}$  is needed to make a  $D_{\text{crat}} > 300 \text{ km}$  diameter basin [30] with the velocities from Fig. S1. The current main belt has  $\sim 7500$  such asteroids [18]. The main belt just prior to the LHB was  $\sim 4$

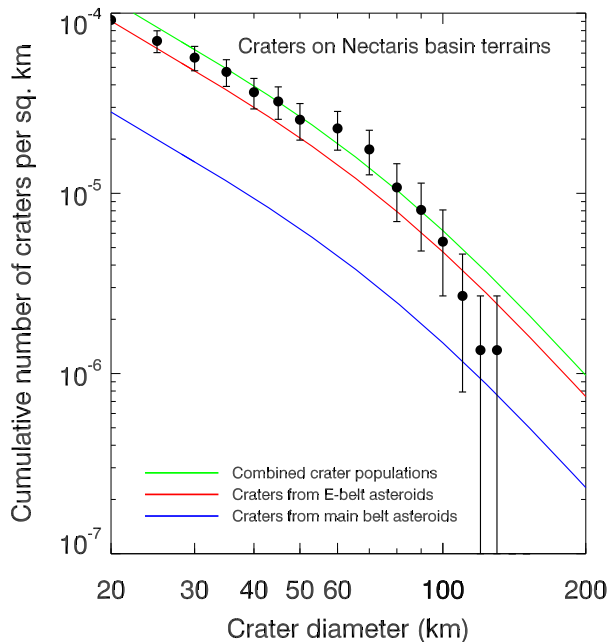


Figure S2: A comparison between observed and model craters formed on terrains affected by Nectaris basin, which may have formed close to the start of the LHB. The black points represent craters counted using Lunar Orbiter Laser Altimeter data (see [28] for details). Error bars correspond to the square root of the count (Poisson statistics) for each bin. The model craters come from the E-belt (red curve) and main belt (blue curve). The green curve shows both populations combined together.

times its current size, with  $\sim 50\%$  pushed out during the LHB [11, 12] and another  $50\%$  lost via dynamical diffusion in the LHB's aftermath (e.g., objects suddenly found themselves embedded within resonances) [13]. Numerical simulations indicate that  $0.015\%$  of those bodies should end up hitting the Moon [13].

**LHB-era lunar basins from the E-belt.** The number of lunar basins formed by our  $e_{\max}^{\text{Mars}} = 0.025, 0.05, 0.12,$  and  $0.17$  runs was calculated as follows. First, we estimated the E-belt populations that existed just prior to the LHB by combining our decay rate results from Fig. 2 in the main text with the present-day Hungaria population calculated above. This yielded  $0.8 \pm 0.4, 0.6 \pm 0.3, 0.2 \pm 0.1,$  and  $0.4 \pm 0.2$  times the present-day main belt population, respectively.

Next, we determined the fraction of our E-belt test bodies that hit the Earth, and scaled that value to the Moon by estimating the ratio of gravitational cross-sections of the Earth and Moon for E-belt encounter velocities (Fig. S1). For the latter, we found that for every  $\sim 17$  objects that hit Earth, one hits the Moon. Thus, the fraction of the E-belt population that hit the Moon during the LHB was  $0.19\%, 0.23\%, 0.18\%,$  and  $0.12\%$  of the pre-LHB population, respectively. These results yield  $10 \pm 5, 9 \pm 4, 3 \pm 1,$  and  $3 \pm 2$  lunar basins, respectively. We predict that approximately one fourth of the basins should be Imbrium to Orientale-sized ( $D_{\text{crat}} > 900$  km; [2, 3]). By combining the  $e_{\max}^{\text{Mars}} = 0.025$  and  $0.05$  runs to get better impact statistics, we obtain a net fraction of test bodies hitting the Moon of  $0.21\%$  and a mean number of lunar basins formed of  $\sim 9-10$  (with factor of 2 error bars).

## 5 Did the LHB Start Near the Beginning of the Nectarian Era?

### 5.1 Modeling Crater Production on Nectaris Basin

In the main text, we argued that the LHB started near the formation time of Nectaris basin (and the Nectarian era). As a partial test of this idea, we compared observed craters formed on terrains affected by Nectaris basin with prediction from our model results (Fig. S2). Here we combined our  $e_{\max}^{\text{Mars}} = 0.025$  and 0.05 runs with the following components: the main belt's current size-frequency distribution [18]; the E-belt and main belt populations just prior to the LHB, set at 0.7 and 4 times the current main belt population, respectively [11, 12, 13]; the fraction of LHB-era objects lost from each population, 99.9% and 75%, respectively; the LHB-era collision probabilities of E-belt and main belt objects with the Moon, estimated from impacts in our runs to be 0.21% and 0.015%, respectively; lunar impact velocities of 21 and 20 km/s, respectively; and crater-scaling relationships suitable for the Moon [30].

Our work shows a reasonable match between model and observations. This does not prove the LHB started near Nectaris, but it does provide an useful consistency check for our predictions.

### 5.2 Additional Evidence From Lunar Craters and Basins

It is challenging to interpret the ancient impact record of the Moon in a quantitative manner. First of all, the Moon is believed to have been produced in a giant impact  $60_{-10}^{+90}$  My after the first solids formed [47], a somewhat broad interval in time. Second, the Moon has been bombarded incessantly by multiple small body populations since its formation (e.g., [48]). Some potential impactor populations include leftover planetesimals in the terrestrial planet region, asteroids residing near or ejected from the E-/main asteroid belts, and comets that were driven into the inner solar system by various dynamical processes. The initial states of these populations, produced by planet formation processes, are at best only partially understood at this time. Third, all of these populations were affected by collisional and dynamical evolution, which may have significantly modified their SFDs over time (e.g., [18, 27, 49]). Fourth, the ages of the oldest recognizable basins and craters on the Moon are indeterminate, with the most ancient well-defined pre-Nectarian basins potentially only going back as far as the closure age of the lunar crust (e.g., possibly as young as 4.3 Ga; [50]).

To all of this, we now add one more complication. Many previous investigations of early lunar impactor populations assumed the giant planets formed on their present-day orbits (e.g., [27]). If the Nice model is correct, however, the giant planets originally formed in a more compact configuration, with eccentricities and inclinations much lower than their current values ([10, 12, 32]; see also main text). Numerical modeling work by our team suggests these kinds of planetary systems produce less dynamical excitation among test bodies residing in the inner solar system than the current configuration of planets. This likely explains why the median impact velocities of E-belt projectiles striking the Moon went from  $V = 9 \text{ km s}^{-1}$  prior to late giant planet migration to  $21 \text{ km s}^{-1}$  in the current system of planets (Fig. S1).

Intriguingly, a significant increase in lunar impact velocities should produce substantially larger basin/crater sizes as one moves from the oldest to moderately younger terrains. The identification of this putative change would be exciting in a number of ways. First, it would lend support for the idea of late giant planet migration, since this mechanism can potentially boost lunar impact velocities. Second, it would potentially tell us when late giant planet migration started, at least in terms of the ages of lunar morphology. Third, it would suggest the lunar impactor population prior to giant planet migration was dominated by projectiles that hit at relatively low velocities. This could potentially act as a constraint to rule out planet formation models that produce overly-excited lunar impactor populations. Conversely, if a crater size change was not

observed, it might be used as a strike against the Nice model, though an alternative could be that early lunar impact populations had such high eccentricities and inclinations that they were relatively unaffected by giant planet migration.

**Crater evidence for the onset of the LHB.** The search for a velocity change signal in lunar crater SFDs was recently undertaken by [28]. They found, using new counts of 15 – 150 km diameter craters, that the crater SFDs on terrains on or near Nectaris basin, roughly the twelfth youngest lunar basin, were similar in shape to those on ancient Pre-Nectarian terrains, but the craters themselves were 30-40% larger. These results were used to derive the size of a characteristic inflection point, or elbow, in the crater SFDs ( $D_{\text{elbow}}$ ). For those projectiles that produced early Pre-Nectarian craters,  $D_{\text{elbow}} = 45$  km, while for those made on younger terrains near Nectaris,  $D_{\text{elbow}} = 60$  km. Pi-group crater-scaling relationships [30] indicate that crater diameter is  $\propto V^{0.44}$ . Thus, the shift in  $D_{\text{elbow}}$  corresponds to a factor of  $\sim 2$  increase in impact velocity (i.e.,  $= (60/45)^{1/0.44}$ ).

The results of [28] imply that giant planet migration took place near the formation time of Nectaris basin. The factor of  $\sim 2$  increase in lunar impact velocities also matches predictions from Fig. S1, which could suggest asteroids residing near or ejected from the E- and main belts were an important source of Pre-Nectarian craters together with leftover planetesimals from the inner solar system. A potential problem with this idea, however, is that these primordial asteroid populations may not lose enough objects at the right times to produce the observed Pre-Nectarian craters.

Consider that the number of  $D > 20$  km craters found on the most ancient lunar surfaces is  $2\text{-}3 \times 10^{-4} \text{ km}^{-2}$ , while those on terrains near Nectaris basin are  $1 \times 10^{-4} \text{ km}^{-2}$  [28] (see also Fig. S2). This means the number of Pre-Nectarian impactors produced by asteroids had to be roughly equivalent to those produced during Nectarian era, when presumably most E- and main belt asteroids were presumably ejected by sweeping resonances via late giant planet migration. While numerical tests do suggest collision probabilities between ejected asteroids and the Moon were a factor of a few higher in the pre-LHB than during the LHB, our back of the envelope tests still appear to be a factor of several away from what is needed. This opens the door for leftover planetesimals in the terrestrial planet region, which may produce many Pre-Nectarian impactors. We consider this a fascinating possibility because at least some of these impactors would have to remain in a modestly-excited state until the Moon's crust solidified, potentially hundreds of My after the Moon formed.

**Basin evidence for the onset of the LHB.** Given the findings of [28], we find it plausible that the lunar basin record might also show signs for a increase in impactor velocities. To investigate this, we examined the basin data set described by [2], which contains 44 basins divided into 14 relative age groups, with 1 being the youngest basin Orientale and 14 being the oldest basin South Pole-Aitken basin. D. Wilhelms [2] placed basins with similar relative ages into several distinct age groups (i.e., 8 basins in group 4, 4 basins in group 5, 2 basins in group 6, 4 basins in group 8, 2 basins in group 10, 3 in group 11, 6 in group 12, and 9 in group 13). Here we sorted the basin data by age and then calculated a running mean of basin diameter, using a window of five individual diameter values. The order of individual basins within distinct age groups were randomized and rerun with our model multiple times, with no significant changes observed. We also ran tests where all but three of the basins in group 13 were eliminated; most cannot be identified in Clementine or LRO images (P. Spudis, personal communication). Once again, no significant changes to the main trends were observed.

Our results are shown in Fig. S3a. The open stars are the sizes of the 44 basins. The filled stars show running mean values, with the vertical bars representing  $1 \sigma$  error bars in diameter and the horizontal bars showing the width of the running mean. While the data should be treated cautiously, particularly because we are dealing with small number statistics, we find that, by eye, the mean basins in the middle to late Pre-Nectarian are distinctly lower than those of the Nectarian, with a step function transition taking place

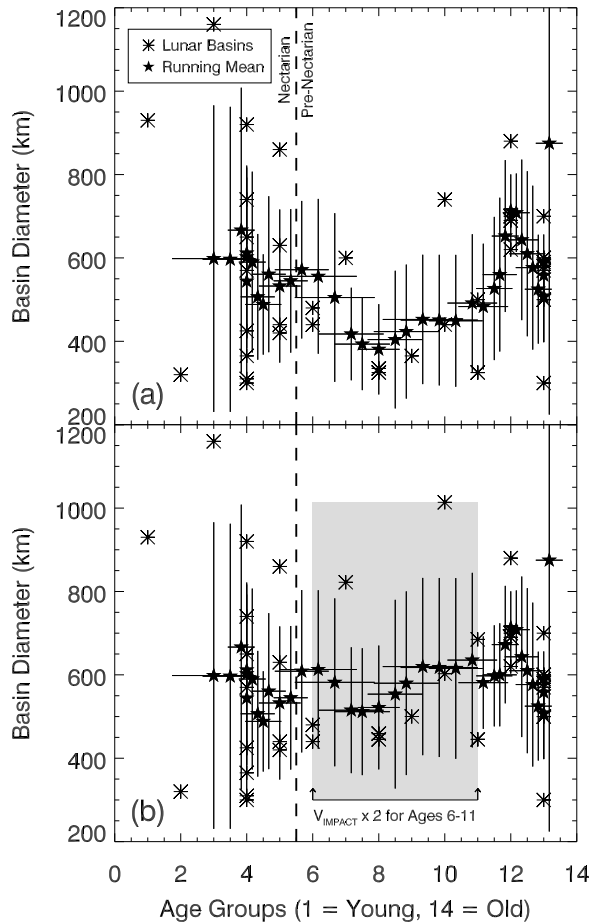


Figure S3: A running mean of lunar basin diameters as a function of relative age. (a) Here 44 lunar basins, plotted as open stars, have been placed into 14 relative age bins, with 1 being the youngest (Orientale) and 14 being the oldest (South Pole-Aitken) [2]. The running mean window was 5 basin diameters. The horizontal error bars show the running mean window, while the vertical error bars show the  $1\sigma$  error bars in diameter. The time between the Nectarian and Pre-Nectarian-eras is shown by the dashed line. The running mean undergoes a transition near the dashed lines, with younger Pre-Nectarian basins being smaller on average than Nectarian basins. (b) Here the basins with ages between 6-11 have been increased in size by a factor of 1.4. This corresponds to increasing the impact velocity by a factor of 2. The Nectarian and Pre-Nectarian basins now show little in the way of a transition near the dashed lines.

near the boundary of those eras. This is surprisingly consistent with the predictions of our model and those of [28].

For Fig. S3b, we increased the sizes of the middle to late Pre-Nectarian basins (age groups 6-11) by a factor of 1.4, which corresponds to increasing their impact velocity by a factor of  $\sim 2$  (see above). The new mean diameter values, shown in the gray rectangle, now appear consistent with the younger Nectarian-era basins, and the transition near the dashed line is largely eliminated. Interestingly, the basins in age groups 12-13 do not fit this pattern. We hesitate to say much about this, given the quality of the data and how little is known about the oldest basins, but it will be interesting to see if data from the GRAIL mission produces comparable trends.

Overall, given the somewhat crude methods used to produce Fig. S3, we do not consider the basin trends more than mildly encouraging, but they do serve as an interesting consistency check. Together with the results of [28], they may suggest that a late planet migration starting time near the formation time of Nectaris basin has merit.

## 6 Thoughts on the Original Composition of the E-Belt

The precise nature of the E-belt is forever lost to us, with 99.9% or more of its starting population eliminated by collisional and dynamical processes (see main text). Still, it is interesting to briefly speculate about its original make-up by piecing together the available information.

The trends of the main asteroid belt today suggest a broad-scale taxonomic stratification among its largest bodies. S-type asteroids, believed to be analogous to a range of metamorphosed meteorites and ordinary chondrites, dominate the inner main belt, while C-type asteroids, believed to be analogous to carbonaceous chondrites, dominate the outer main belt [51, 52, 53]. Additional trends, such as the inclusion of P- and D-type asteroids in the outer main belt, Hilda, and Trojan populations, may come from the injection of dormant comets from the primordial disk during the Nice model [38]. Thus, from a planetesimal perspective, we expect more processed, metamorphosed material as we move closer we get to the Sun [49].

At the time of the LHB, the E-belt at the inner edge of the main belt was the closest stable reservoir of small bodies (that we know of) to the terrestrial planet region. If there was mixing of planetesimals from different zones by early solar system processes, such as planet migration or the scattering of planetesimals by embryos (e.g., [49, 54, 55]), the E-belt was probably a repository of leftover planetesimal fragments from the terrestrial planet region. Accordingly, it is useful to examine the kinds of planetesimals needed to make Earth and Mars.

Oxygen isotope systematics have previously been used to roughly determine the kinds of meteorite classes needed to make Earth and Mars [56, 57] (see also [58]). These techniques suggest reasonable matches to the Earth-Moon system come from a combination of enstatite and ordinary chondrite-like planetesimals ( $\sim 90\%$ ) combined with a smaller fraction of carbonaceous chondrite-like materials ( $\sim 10\%$ ): 70% EH-, 21% H-, 5% CV-, and 4% CI-chondritic material. For Mars, enstatite chondrite-like material is replaced by ordinary chondrite-like material, though  $\sim 15\%$  still has to come from carbonaceous chondrite-like materials: 85.4% H-, 10.9% CV-, and 3.6% CI-chondritic material. Intriguingly, the largest component of carbonaceous material for Earth and Mars comes from (metamorphosed) CV chondrites. These values should not be accepted literally, given the numerous constraints needed to make Earth and Mars, but they do provide some insights into the kinds of things that once existed in the terrestrial planet region.

If mixing of inner solar system planetesimals was once important, it seems probable that the E-belt once contained enstatite chondrite-like objects, ordinary chondrite-like objects, CV-chondrites, and perhaps a dash of primitive CI- or CM-like objects. Given the expected degree of collision evolution in the inner solar system, we would predict many E-belt objects were originally fragments of larger planetesimals, with some potentially coming from partially- or completely differentiated parent bodies [49]. This would be consistent with the idea that planetesimals formed nearer the Sun have faster accretion times and are more affected by quickly-decaying radiogenic heat sources like  $^{26}\text{Al}$  and  $^{60}\text{Fe}$ .

Examining the known Hungarias, we find the background population is dominated by small E/X- and S-type asteroids. These objects may be analogous to the enstatite and ordinary chondrite-like materials needed to make Earth and Mars. Moreover, observations of (21) Lutetia by the Rosetta mission also hint at interesting connections between enstatite and CV chondrites, as well as the possibility that Lutetia came from a partially differentiated parent body (e.g., [59]). Thus, we find it plausible some of the E- and X-type asteroids found in the Hungaria population have affinities for CV-chondrites. Adding to the confusion, K-type asteroids may also be a plausible source of CV or other kinds of carbonaceous chondrites [60], and this class shares spectral similarities in the near-IR with S-type asteroids. Collectively, these data imply we still have much to learn about the true nature of planetesimal formation and evolution in the inner solar system.

The highly siderophile element abundances of LHB-era projectiles hitting the Moon also appear to be broadly consistent with the compositions above, with iron and enstatite chondrite-like projectiles potentially

producing the Imbrium and Serenitatis basins, respectively (see Sec. 1). Comparable results come from the chromium content and isotopic signatures of material found in Archean-era impact spherule beds found on Earth. The oldest known Archean spherule beds look like they were produced by metamorphosed carbonaceous chondrites, with the closest match being to CV chondrites (or in some cases, CK or CR chondrites) [5, 61]. The younger Archean and early-Proterozoic spherule beds look like they were produced by enstatite and ordinary chondrite-like projectiles [62]. All of these compositions fit with the kinds of planetesimals needed to make Earth and Mars.

Note that differences exist in inferred projectile compositions between some of the ancient Archean spherule beds and the younger Archean and early-Proterozoic beds. The origin of this difference is unclear to us. If it turns out to be robust, it could suggest some degree of compositional zoning within the initial E-belt itself, with some zones more likely to produce impactors at given times than others. Our modeling results suggest this scenario may be possible, but we have yet to explore this issue in detail. Alternatively, it could point to collisional or even tidal disruption (via planetary encounters) among members of the destabilized population, with fragments from a large breakup event potentially dominating the terrestrial impactor flux for a given interval. The connection between these different impact bed signatures will be interesting to investigate in the future.

## 7 Frequently Asked Questions About Impact Spherule Beds

Terrestrial impact spherule beds are intrinsically interesting to those that want to understand the history of the Earth. We encourage those readers who want to know more about them to explore these papers [4, 5, 6, 8, 9] and the references therein. Here we address several frequently asked questions that have come up about impact spherule beds that may be of general interest.

### Q: Does it make sense to have numerous impact spherule beds in the Archean era?

We believe the answer is yes. As discussed in the main text, the Moon has three Chicxulub-sized or larger craters that formed in the Late Imbrian era (3.2-3.7 Ga), and perhaps one that formed in the Eratostenian era (1.5-3.2 Ga). For the present-day Earth-crossing object population, we know that the ratio of the gravitational cross-sections of the Earth and Moon is approximately 17-20 (i.e., for every object that strikes the Moon, seventeen to twenty or so should strike the Earth), and that a typical impactor hitting either body near its mean velocity ( $\sim 20 \text{ km s}^{-1}$ ) will produce final craters that are comparable in size to one another [16, 30]. Accordingly, even if the model presented in the main text is wrong, the values above allow us to say the following:

- It is **unavoidable** that on the order of  $\sim 70$  impactors capable of making Chicxulub-sized craters hit the Earth over the Archean and possibly the early Proterozoic periods.
- If the impactor size-frequency distribution was comparable to the observed one in the main asteroid belt, we can infer that a substantial fraction of Archean-era impactors produced craters as large as the Nectarian- and Imbrian-era basins observed on the Moon. In fact, a few of these events should have rivaled those that produced Imbrium and Orientale basin on the Moon.

Given the number and size of these events, and the fact that the impactor that formed Chicxulub crater also made an impact spherule layer that was up to 0.2-0.5 cm thick [6], we find it highly plausible that at least some traces of these Archean-era impacts were left behind in the surviving strata.

## Q: Why have impact spherule beds not been found in other Archean times beyond those reported in the text?

We attribute the lack of reports of spherule layers from  $\sim 2.7$  to 3.1 Ga to a combination of lack of preservation and lack of effort expended to find them. Consider the following:

- Archean rocks of any sort are scarcer than rocks of any other age.
- Only a fraction of the surviving Archean rocks are strata that were deposited in environments where spherule layers could be captured and preserved (e.g., shales deposited below the wave base do a good job of preserving spherule beds) [63].
- The aggregate area of the Archean-era continents, and hence their shelves and slopes, was probably smaller during the Archean than later in Earth history.
- Most Archean rocks have been metamorphosed, and once they are, original features such as spherules cannot be recognized.
- Few geologists are currently looking for spherule layers. In general, impact evidence is not on the standard geologist's "checklist" of things to look for, and one cannot distinguish impact spherules from other spherical bodies like accretionary lapilli and oolites without careful inspection [64].
- Almost all of the well-preserved sedimentary and volcanic rocks from the 3.24-3.47 and 2.49-2.63 Ga windows are found either in the Pilbara Craton of Western Australia or the Kaapvaal Craton of South Africa. These two areas are where all of the known Archean spherule layers have been found. They are also where a disproportionately high share of the high-resolution studies of Earth's Archean surface environments and biotas have been done. These two cratons were apparently unusually stable because few if any other blocks of Archean crust found to date were as successful at avoiding tectonic deformation. Even on these two cratons, few unmetamorphosed strata deposited between 2.63 and 3.24 Ga have been found.
- Even in well-preserved strata from appropriate environments, the search for impact spherule beds is far from easy (e.g., co-author B. Simonson and co-workers have been studying the 2.49-2.63 Ga strata of Western Australia since 1985 and so far have only found layers from 4 impacts [8, 62]).

Taken together, we believe it is not surprising that layers have yet to be reported in other terrains. We fully expect that many additional layers will be found in other spans of Archean time if suitable strata can be found and studied with the same level of intensity.

## Q: How do we infer that the Archean impact spherule beds were globally distributed?

The surviving Archean spherule layers are locally preserved scraps of layers, but the easiest way to explain their characteristics is if they were once globally distributed. This inference is based on many favorable points of comparison between the Archean layers and ejecta from two well-documented Phanerozoic examples of global ejecta layers: the K-Pg layer and an Eocene layer rich in microkrystites (e.g., [9]). They were presumably produced by the 180 km diameter Chicxulub crater and the 100 km diameter Popagai crater, respectively.

The main way in which the Archean layers are not comparable to the Phanerozoic examples is the fact that they are thicker within a given area [65] and have characteristic spherule sizes that compare favorably

with major impacts [4]. Intuitively, this leads to the conclusion that the impacts that made them were as large or larger than those of the Phanerozoic (e.g., Chicxulub). Additional evidence suggests this conclusion is correct. For example, the fluence of Ir in some of the early Archean layers exceeds that of the K-Pg ejecta layer [61, 66].

### **Q: Why do the Archean impact spherule beds lack some of the shocked materials associated with those that go with the well-studied Chicxulub crater event?**

Longer discussions of the absence of shocked quartz in Archean layers can be found in [5] and [67]. We summarize the essential arguments here.

- **Target composition.** If continents were smaller in the Archean, oceanic crust would have covered a larger fraction of the Earth's surface than it does today. Therefore, a larger fraction of Archean impacts would have taken place in mafic rocks instead of hitting granitic continental crust like the Chicxulub and Sudbury impacts. Impacts in mafic target rocks such as oceanic crust will not produce shocked quartz crystals. Therefore, the extreme scarcity of shocked quartz in Archean spherule layers may reflect a secular change in the Earth's crust [68].
- **Diagenetic alteration.** Quartz is more resistant to both physical erosion processes and chemical alteration than any other common mineral. This is why quartz eventually dominates the mineralogy of sandstones if such processes keep attacking the sand grains. Even shocked grains of quartz are surprisingly resilient during erosion and can be transported for significant distances [69]. In contrast, while the main phases in mafic rocks (calcic plagioclase, pyroxene, and olivine) are commonly transported as heavy minerals, they are among the phases most easily replaced during diagenesis. There is abundant textural evidence in the Archean layers that minerals other than quartz (including plagioclase, pyroxene, and olivine) were originally present in the spherules and among associated grains and have since been replaced [5, 8, 64, 66]. Even in the K-Pg layer, clinopyroxene crystals in distal spherules rarely escaped diagenetic replacement [70, 71].
- **Impact size.** The larger an impact, the greater the fraction of the disturbed target rock that is melted or vaporized [72]. Typically, distal ejecta from large impacts contain a high ratio of formerly molten or vaporized material (especially spherules) to unmelted material such as shocked mineral grains [73].

In summary, given the possible differences in average size and target material composition between Archean and Phanerozoic impacts, the scarcity of shocked minerals in the Archean spherule layers may not be surprising.

### **Q: Are the spherule beds likely to be volcanic in origin?**

We believe this is unlikely. Some Archean layers have a chondritic component that makes up roughly half the mass of the spherules (e.g., the early Archean S3 and S4 layers [74] and the late Archean Paraborudoo and Reivilo layers [75]). We believe a chondritic component rules out a volcanic origin for the layers, even though melt spherules are present in certain types of volcanic deposits.

The hypervelocity impact of a body like an asteroid seems the easiest way to create a thin yet regionally extensive layer, half of which came from space yet encased in strata (e.g., shales) that lack any detectable chondritic material. The only potential alternative to a large impact would be an undiluted accumulation of cosmic dust. The amount of time it would take to accumulate enough dust to reach the measured thicknesses

of the Archean layers is far too long to represent a realistic hiatus in sedimentation in a shale-depositing environment. Even if it this was not true, this scenario offers no explanation for the abundance of sand-size spherules that were formerly molten.

**Q: Should we expect to see a wide range of differences in the content of chondritic materials within different Archean spherule layers?**

Yes. Consider the following.

- The K-Pg layer shifts downrange over thousands of kilometers from Platinum-group element (PGE)-poor melt spherules (emplaced ballistically close to Chicxulub) to distal spherules that are much richer in PGEs (because they incorporated much higher fractions of material from the impactor) [71]. By analogy, one could read the variations in the levels of chondritic material in different Archean spherule layers as reflecting the fact they were captured and preserved at different distances from the point of impact (scaled to crater radii). The varying concentrations of PGEs could then reflect differences in the amounts of vaporized impactor incorporated into the spherules.
- Impactors vary in composition. Average values are used to calculate chondritic content, but some natural variation about the mean is to be expected. Impact melts are themselves quite heterogeneous from the intrinsic messiness of the process.
- At least some PGEs are more highly mobile in certain diagenetic situations than others (e.g., the study of the Acraman ejecta layer by [76]).

**Q. Why are the primary signs of Archean impacts distal ejecta rather than impact structures or proximal ejecta?**

Major impact events, like those that produced Chicxulub, produce distal ejecta layers that cover orders of magnitude more area than the impact crater or even the proximal ejecta, defined technically as all of the ejecta within 5 crater radii of the impact [73]. This implies that large Archean events that produce globally-distributed ejecta are favored by preservation bias, with their distal ejecta more likely to be captured in a preservation-friendly zone than that from smaller impacts.

If the Archean spherule layers were generated by oceanic impacts, as seems likely, their source craters were probably subducted long ago. This would help explain why clear signs of shock metamorphism have yet to be found in Archean rocks (with the possible exception of crystals in a few spherule layers [77, 78]). It is also likely that the size of impact structures as large as Chicxulub would be very difficult to determine in Archean cratons given the high level of tectonic deformation and deep erosion typical of such areas.

Moreover, in some ways, it is easier to preserve recognizable distal ejecta layers in the Precambrian than it was in the Phanerozoic. For example, distal ejecta layers could get dispersed by burrowing animals in the Phanerozoic but not in the Precambrian. Spherules deposited on the seafloor may also have dissolved more readily in the Phanerozoic because silica concentrations are low in modern seawater, but Precambrian seawater was saturated with silica [79, 80]. For all these reasons, we believe distal ejecta layers are much likelier to provide a tangible record of large Archean impacts than impact structures.

## Q. Why are so few impact spherule layers associated with Phanerozoic craters?

Most of the  $\sim 180$  known impact structures, nearly all which formed within the Phanerozoic, or approximately the last 542 My, were probably too small to generate sizable global ejecta layers. While the precise impactor size needed to make a thick global spherule bed is unknown, most Archean beds are as thick as or thicker than those associated with the 65 My old, 180 km Chicxulub crater. In comparison, the 35 My old, 100 km Popigai crater, perhaps the second largest crater known from the Phanerozoic, made a distal spherule bed that is least one (and possibly three) orders of magnitude thinner than the K-Pg layer [6, 65]; we consider it unlikely it would be detected on more ancient terrestrial terrains.

It is possible that some Chicxulub-sized craters formed over the Phanerozoic have either been erased by geologic processes or they have yet to be detected. This raises the possibility that extensive searches may yet yield some new impact spherule beds over the Cambrian era. While we look forward to new beds being discovered, we are unsure how many should exist *a priori*.

The rate of Chicxulub-sized impact events over the last  $\sim 600$  My is poorly known. It is predicated on precise knowledge of the asteroid belt, particularly family-forming events in the inner main belt that can produce Chicxulub-sized projectiles, as well as the escape route and rate that such objects make it into the inner solar system. At present, we can only say the following. The orbital and size distribution of the present-day near-Earth object population suggests the interval between Chicxulub-sized impacts is perhaps between 350 to 1000 My [11, 81]. Thus, it is entirely possible that the Chicxulub event was the largest of the Phanerozoic era.

## 8 Compendium of Useful Events and Numbers From Text

- **Geologic periods on the Earth.** Archean Period (2.5-3.7 Ga). Proterozoic Period (0.6-2.5 Ga).
- **Ancient impact spherule beds on Earth.** These beds span the Archean and early Proterozoic. There are at least 7 beds between 3.23-3.47 Ga, 4 beds between 2.49-2.63 Ga, and 1 bed between 1.7-2.1 Ga.
- **Ancient craters on Earth.** Sudbury crater is 250 km diameter across and is 1.85 Ga. The size of Vredefort crater is debated, but it is at least 180 km and possibly 300 km in diameter. Vredefort is 2.023 Ga.
- **Geologic periods on the Moon.** Assuming our model results are correct, we predict the Pre-Nectarian period extended from the origin of the Moon to 4.1-4.2 Ga, a potential age for Nectaris basin. The Nectarian period spans 4.1-4.2 Ga to approximately 3.8-3.9 Ga, the likely age of Imbrium basin derived by Apollo samples and lunar meteorites. The Lower or Early Imbrian period is from 3.8-3.9 Ga to 3.7-3.8 Ga, the estimated age of Orientale basin. The Upper or Late Imbrian period is from 3.7-3.8 Ga to 3.2 Ga. The Eratosthenian period is from 3.2 to 1.5 Ga, though the precise time of the younger boundary age is debated.
- **Large late craters on the Moon.** For the Late Imbrian era (3.2-3.7 Ga), the Iridium, Humboldt, Tsiolkovskiy craters are 260, 207, and 180 km in diameter, respectively. For the Eratosthenian era (1.5-3.2 Ga), the Hausen crater is 167 km in diameter. Note that Hausen crater may also be from the Late Imbrian era.
- **Chronology of shock degassing ages.** The ancient  $^{39}\text{Ar}$ - $^{40}\text{Ar}$  shock degassing age profiles from HEDs, presumably from (4) Vesta, the H chondrites, and many ancient lunar rocks returned by the

Apollo 16 and Luna 20 missions are surprisingly similar to one another. The listed meteorites above yield a spike of ages near 4.5 Ga, few ages between  $\sim 4.1$ -4.4 Ga, and numerous ages between  $\sim 3.5$ -4.1 Ga. The lunar samples yield few  $^{39}\text{Ar}$ - $^{40}\text{Ar}$  ages older than 4.1-4.2 Ga and numerous ages between 3.7-4.1 Ga.

- **Inferred timing of major events. 4.52-4.45 Ga.** Formation of Moon. **4.3-4.4 Ga.** Closure of lunar crust, and possible start of recorded Pre-Nectarian crater record. Most impacts produced by leftover planetesimals and asteroid refugees from the E- and main belts. **4.1-4.2 Ga.** Start of LHB. Late migration of giant planets. Dispersal of primordial comet disk. Ejection of material from the primordial main belt. Destabilization of the E-belt. Formation of Nectaris basin. **3.7-3.8 Ga.** Formation of Orientale basin on Moon. End of basin-forming era on Moon. **2.5 Ga.** End of basin-forming era on Earth. **1.7-1.8 Ga.** Approximate end of production of Chicxulub-sized craters on Earth from E-belt projectiles.

## References

- [32] Nesvorný, D. Young solar system's fifth giant planet? *Ap. J. Lett.* **742**, L22 (2011).
- [33] Morbidelli, A., Levison, H. F., Tsiganis, K., & Gomes, R. Chaotic capture of Jupiter's Trojan asteroids in the early Solar System. *Nature* **435**, 462-465 (2005).
- [34] Nesvorný, D., & Vokrouhlický, D. Chaotic capture of Neptune Trojans. *Astron. J.* **137**, 5003-5011 (2009).
- [35] Levison, H. F., Morbidelli, A., Van Laerhoven, C., Gomes, R., & Tsiganis, K. Origin of the structure of the Kuiper belt during a dynamical instability in the orbits of Uranus and Neptune. *Icarus* **196**, 258-273 (2008).
- [36] Nesvorný, D., Vokrouhlický, D., & Morbidelli, A. 2007. Capture of irregular satellites during planetary encounters. *Astron. J.* **133**, 1962-1976 (2007).
- [37] Bottke, W. F., Nesvorný, D., Vokrouhlický, D., & Morbidelli, A. The irregular satellites: The most collisionally evolved populations in the solar system. *Astron. J.* **139**, 994-1014 (2010).
- [38] Levison, H. F., Bottke, W. F., Gounelle, M., Morbidelli, A., Nesvorný, D., & Tsiganis, K. Contamination of the asteroid belt by primordial trans-Neptunian objects. *Nature* **460**, 364-366 (2009).
- [39] Minton, D. A., & Malhotra, R. A record of planet migration in the main asteroid belt. *Nature* **457**, 1109-1111 (2009).
- [40] Levison, H. F., Morbidelli, A., Vokrouhlický, D., & Bottke, W. F. On a scattered-disk origin for the 2003 EL<sub>61</sub> collisional family—An example of the importance of collisions on the dynamics of small bodies. *Astron. J.* **136**, 1079-1088 (2008).
- [41] Weissman, P. R., Asphaug, E., & Lowry, S. C. Structure and density of cometary nuclei. In *Comets II*, (eds. Festou, W. F. et al.), 337-357 (University of Arizona Press, 2004).
- [42] Levison, H. F., Morbidelli, A., Dones, L., Jedicke, R., Wiegert, P. A., & Bottke, W. F. The mass disruption of oort cloud comets. *Science* **296**, 2212-2215 (2002).
- [43] Chapman, C. R., Cohen, B. A., & Grinspoon, D. H. What are the real constraints on the existence and magnitude of the late heavy bombardment? *Icarus* **189**, 233-245 (2007).

- [44] Haskin, L. A., Korotev, R. L., Rockow, K. M., & Jolliff, B. L. The case for an Imbrium origin of the Apollo Th-rich impact-melt breccias. *Meteoritics and Planetary Science* **33**, 959-975 (1998).
- [45] Swindle, T. D., Isachsen, C. E., Weirich, J. R., & Kring, D. A.  $^{40}\text{Ar}$ - $^{39}\text{Ar}$  ages of H-chondrite impact melt breccias. *Meteoritics and Planetary Science* **44**, 747-762 (2009).
- [46] Durda, D. D. *et al.* Size-frequency distributions of fragments from SPH/N-body simulations of asteroid impacts: Comparison with observed asteroid families. *Icarus* **186**, 498-516 (2007).
- [47] Touboul, M., Kleine, T., Bourdon, B., Palme, H., & Wieler, R. Late formation and prolonged differentiation of the Moon inferred from W isotopes in lunar metals. *Nature* **450**, 1206-1209 (2007).
- [48] Bottke, W. F., Walker, R. J., Day, J. M. D., Nesvorný, D., & Elkins-Tanton, L. Stochastic late accretion to Earth, the Moon, and Mars. *Science* **330**, 1527 (2010).
- [49] Bottke, W. F. *et al.* Iron meteorites as remnants of planetesimals formed in the terrestrial planet region. *Nature* **439**, 821-824 (2006).
- [50] Elkins-Tanton, L. T., Burgess, S., & Yin, Q.-Z. The lunar magma ocean: Reconciling the solidification process with lunar petrology and geochronology. *Earth and Planetary Science Letters* **304**, 326-336 (2011).
- [51] Burbine, T.H., McCoy, T.J., Meibom, A., Gladman, B., & Keil K. Meteoritic parent bodies: Their number and identification. In *Asteroids III* (eds. Bottke, W. F. *et al.*), 653-667 (University of Arizona Press, 2002).
- [52] Gradie, J., & Tedesco, E. Compositional structure of the asteroid belt. *Science* **216**, 1405-1407 (1982).
- [53] Grimm, R.E., & McSween, H.Y. Heliocentric zoning of the asteroid belt by aluminum-26 heating. *Science* **259**, 653-655 (1993).
- [54] Petit, J., Morbidelli, A., & Chambers, J. The primordial excitation and clearing of the asteroid belt. *Icarus* **153**, 338-347 (2001).
- [55] Walsh, K. J., Morbidelli, A., Raymond, S. N., O'Brien, D. P., & Mandell, A. M. A low mass for Mars from Jupiter's early gas-driven migration. *Nature* **475**, 206-209 (2011).
- [56] Lodders, K. An oxygen isotope mixing model for the accretion and composition of rocky planets. *Space Sci. Res.* **92**, 341-354 (2000).
- [57] Lodders, K., & Fegley, B. An oxygen isotope model for the composition of Mars. *Icarus* **126**, 373-394 (1997).
- [58] Burbine, T. H., & O'Brien, K. M. Determining the possible building blocks of the Earth and Mars. *Meteoritics and Planetary Science* **39**, 667-681 (2004).
- [59] Weiss, B. *et al.* Possible evidence for partial differentiation of asteroid Lutetia from Rosetta. *Planet. Space Sci.*, in press (2012).
- [60] Clark, B. E., Ockert-Bell, M. E., Cloutis, E. A., Nesvorný, D., Mothé-Diniz, T., & Bus, S. J. Spectroscopy of K-complex asteroids: Parent bodies of carbonaceous meteorites?. *Icarus* **202**, 119-133 (2009).
- [61] KYTE, F. T., Shukolyukov, A., Lugmair, G. W., Lowe, D. R., & Byerly, G. R. Early Archean spherule beds: Chromium isotopes confirm origin through multiple impacts of projectiles of carbonaceous chondrite type. *Geology* **31**, 283 (2003).

- [62] Simonson, B., *et al.* Geochemistry of 2.63-2.49 Ga impact spherule layers and implications for stratigraphic correlations and impact processes. *Precambrian Res.* **175**, 51-76 (2009).
- [63] Taylor, S. R., & McLennan, S. M. *Planetary Crusts: Their Composition, Origin and Evolution.* (Cambridge University Press, Cambridge, UK, 2009).
- [64] Simonson, B. M. Petrographic criteria for recognizing certain types of impact spherules in well-preserved Precambrian successions. *Astrobiology* **3**, 49-65 (2003).
- [65] Glass, B. P., & Simonson, B. M. Distal impact ejecta layers: Spherules and more. *Elements* **8:1**, in press (2012).
- [66] Lowe, D. R., Byerly, G. R., Asaro, F., & Kyte, F. J. Geological and geochemical record of 3400-million-year-old terrestrial meteorite impacts. *Science* **245**, 959-962 (1989).
- [67] Simonson, B. M., Davies, D., Wallace, M., Reeves, S., & Hassler, S.W. Iridium anomaly but no shocked quartz from Late Archean microkrystite layer: Oceanic impact ejecta? *Geology* **26**, 195-198 (1998).
- [68] Simonson, B. M., & Harnik, P. Have distal impact ejecta changed through geologic time? *Geology* **28**, 975-978, (2000).
- [69] Cavosie, A. J., Quintero, R. R., Radovan, H. A., & Moser, D. E. A record of ancient cataclysm in modern sand: Shock microstructures in detrital minerals from the Vaal River, Vredefort Dome, *South Africa Geological Society of America Bulletin* **122**, 1968-1980 (2010).
- [70] Kyte, F. T., Bostwick, J. A., & Zhou, L. The Cretaceous-Tertiary boundary on the Pacific plate: Composition and distribution of impact debris. In: Ryder, G., Fastovsky, D., & Gartner, S. (eds). *The Cretaceous-Tertiary Event and Other Catastrophes in Earth History. Geological Society of America Special Paper* **307**, 389-401 (1996).
- [71] Smit, J. The global stratigraphy of the Cretaceous-Tertiary boundary impact ejecta. *Ann. Rev. Earth Planet. Sci.* **27**, 75-113 (1999).
- [72] Melosh, H. J. *Planetary Surface Processes* (Cambridge University Press, Cambridge, UK, 2011).
- [73] French, B. M. Traces of catastrophe: A handbook of shock-metamorphic effects in terrestrial meteorite impact structures. *Lunar and Planetary Institute Contribution Number 954*, (Lunar and Planetary Institute, Houston, 1998), 120 pp.
- [74] Kyte, F. T., Zhou, L., & Lowe, D. R. Noble metal abundances in an Early Archean impact deposit. *Geochim. Cosmochim. Acta* **56**, 1365-1372 (1992).
- [75] Goderis, S., *et al.* Geochemical correlation of two late Archean impact spherule layers between South Africa and Western Australia: the Paraburdoo-Reivilo link. *Lunar and Planetary Science Conference* **43**, 1882 (2012).
- [76] Wallace, M. W., Gostin, V. A., & Keays, R. R. Acraman impact ejecta and host shales: Evidence for low-temperature mobilization of iridium and other platoids. *Geology* **18**, 132-135 (1990).
- [77] Rasmussen, B., & Koeberl, C. Iridium anomalies and shocked quartz in Late Archean spherule layer from the Pilbara craton: New evidence for a major asteroid impact at 2.63 Ga. *Geology* **32** 1029-1032 (2004).

- [78] Smith, F. C., Zullo, J. B., Glass, B. P., & Simonson, B. M. Discovery of a shock-induced polymorph of rutile with  $\alpha$ -PbO<sub>2</sub> structure (TiO<sub>2</sub>II) in four Neoproterozoic spherule layers from Western Australia and South Africa. *Meteoritics Planet. Sci.* **45**, A192 (2010).
- [79] Maliva R. G., Knoll, A. H., & Siever, R. Secular changes in chert distribution: A reflection of evolving biological participation in the silica cycle. *Palaios* **4**, 519-532 (1989).
- [80] Siever, R. The silica cycle in the Precambrian. *Geochim. Cosmochim. Acta* **56**, 3265-3272 (1992).
- [81] Bottke, W. F., Vokrouhlický, D., and Nesvorný, D. An asteroid breakup 160 My ago as the probable source of the K-T impactor. *Nature* **449**, 48-53 (2007).